A Need For Speed: Enhancing F1 Race Cars with a Novel Computational Fluid Dynamics and Machine Learning Method

Ken Cheng

Crescent School, Toronto, Ontario, Canada

Abstract. Formula One (F1) engineers dedicate their lives to finding tenths of a second in car performance. But, the technical complexities of F1 cars must now also make inroads to increasing sustainability because fuel consumption in F1 is a major problem. Furthermore, F1 teams with lower budgets now need to find ways to be more efficient in aerodynamic testing to match the richer teams' expensive equipment. This would improve the competitiveness of F1 and please 100 million fans around the world. Computer-aided design to model Formula One race cars for aerodynamic testing, computational fluid dynamics to test 90 different airfoils and simulation setups as well as the finalized model car against the control car, and machine learning to quickly predict the results of other simulations I have not conducted yet with high accuracy rates in a very little amount of time.

Keywords: Computational fluid dynamics, Machine learning, Rear wing, Formula 1, Backpropagation algorithm, Artificial neural networks, Fuel consumption, Drag reduction, Downforce production.

1. Introduction

1.1. Background Information

Formula One (F1) is one of the most highly-regarded, popular, and historic competitions in professional motor racing. Over the span of the 17 F1 Grand Prix (GPs) in 2020, F1 received a cumulative TV audience of about 1.5 billion viewers [1]. F1 drivers are all highly skilled but the majority of success in F1 is attributed to the remarkably fast and technologically advanced cars, making it the most important component of the sport. Although engine power provides the main source of speed for F1 cars, without aerodynamics, a car moving at F1 speeds would be highly inefficient because of the massive amounts of drag slowing it down. Furthermore, the lack of traction from low tire grip stops the car from accelerating as quickly as it could with the integration of high-level aerodynamics onto the car.

So, to not only brake faster but also use higher traction to reach higher cornering speeds, F1 engineers first found in the late 1960s that increasing the downward pressure, or downforce, increased the grip between the wheels and the road, allowing for the most efficient transfer of power generated by the engine to the car's movements on the track. Because of these discoveries, wings were first incorporated into F1 cars in 1968 [2]. Front and rear wings remain one of the most important parts of an F1 car. They are composed of several airfoils set at different angles. Figure 1. shows the components of an F1 rear wing. This project will focus on optimizing the part labelled number 1 in the figure, the main plane.

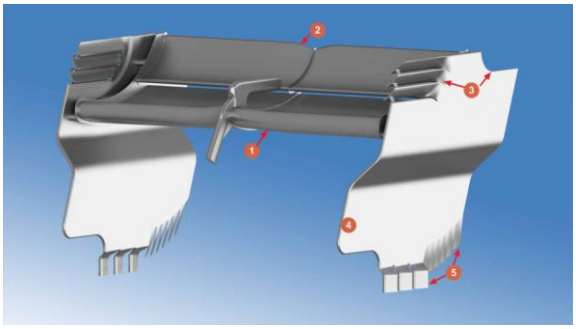

Figure 1. Labeled F1 rear wing (1. Main plane, 2. DRS Flap, 3. Endplates, 4. Middle trim, 5. Bottom trim/Louvers)

Although many unfamiliar with aerodynamics might think that adding components to a car like a rear wing will increase the car's drag, this is incorrect. Turbulent wake regions are formed at the rear end of all cars, negatively impacting aerodynamic performance. However, turbulent wake regions become smaller as airflow is redirected by the rear wing. This reduction also minimizes the pressure differential between the front and back of a car, the source of pressure drag, and thus this lowers the magnitude of pressure drag acting on it.

1.2. Literature Review

Turbulent flow over F1 cars has been a topic that has attracted the attention of many researchers around the world for many years. For example, J. Jagadeep Reddy and Mayank Gupta used CFD to find the optimum angle of attack for the front wing of an F1 car [3]. The paper showed how the drag coefficient (C_D) and lift coefficient (C_L) quantities that quantify the drag and lift of an object in a fluid environment, of front wings varied by their Angle of Attack (AOA), the angle between the airfoil's chord line and the direction of airflow wind, and also determined that the optimum front wing AOA to minimize C_D is at 4º. Even though the paper effectively presented the effects of AOA on C_D, it doesn't talk about the need to examine C_L in the context of F1.

In 2018, Umberto Ravelli and Marco Savini analyzed a simulation of an F1 Car using Open-Source CFD Code and found that the drag force mostly comes from three parts of an F1 car, the rear wing (20.3%), the rear tire (19.5%), and the underbody (15.6%) [4]. Because of these findings, we can see that designing a rear wing that produces as much downforce as possible with as little drag as possible through testing is one of the most vital components in the design of an F1 car. Even though the paper was able to thoroughly discuss the downforce and drag contributing percentages for each part of the car, it only used the 2017 F1 car as a simulation model, and the authors' conclusions about each part of the car might not apply to other models.

1.3. Engineering Goals and Significance of Research

For both passenger cars and racing cars, engine power is used to offset the aerodynamic drag of the car. Racing cars must endure braking and cornering extremities, so intense downforce typically boosts their performance. However, enhanced downforce can also produce a large drag force. So, in the aerodynamic design of the racing car, it is necessary to balance its aerodynamic resistance and aerodynamic downforce.

This project targets the problem of F1 car fuel economy by optimizing the rear wing to both increase the car's overall downforce and substantially minimize its drag. The rear wing was chosen because it contributes 25% of an F1 car's overall downforce and is responsible for 30% of the car's drag, making it crucial to the car's aerodynamic performance. Figure 2. shows what percentage of downforce is gained or lost from each component of an F1 race car as well as a percent distribution of the drag that each component of an F1 race car contributes to the car's overall drag.

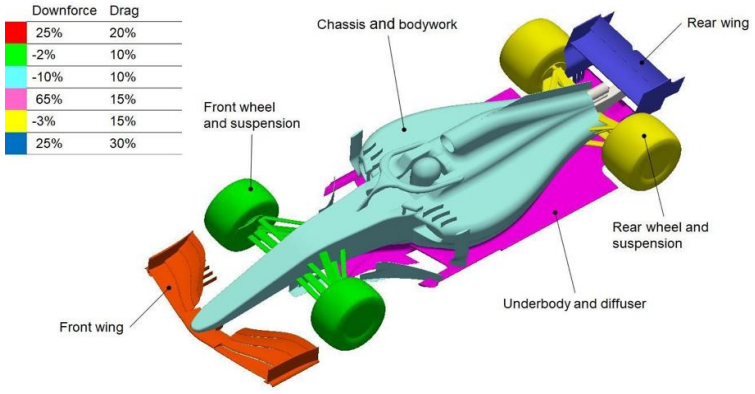

Figure 2. Percentage distributions of drag creation and downforce from each car component

From extensive literature reviews, it is clear that rear wings have a great impact on the aerodynamic performance of an F1 car. But, how and why rear wings can be improved is not clear. To answer these

questions, this project utilizes a novel method in which CFD simulations and a Backpropagation machine learning algorithm work together to optimize rear wing design.

The research has its significance in the following areas: first, the findings will create a better understanding of how rear wings affect flow properties over F1 cars; second, the findings from the testing to find the most optimal rear wing will highlight what factors like camber or thickness are the most important in designing the most optimal rear wing; lastly, the testing to find the most optimal rear wing can also be used to better explain what conditions certain airfoils excel or underperform at.

Also, an F1 car with an optimized rear wing design becomes more efficient and thus more fuel-saving and sustainable, further supporting the global fight against climate change. It will reduce the large carbon footprint that the sport is leaving behind every year. Currently, F1 pollutes the equivalent of powering roughly 30,000 houses in the UK every year [5].

Furthermore, as the sport is making a push to close the performance gap between the best and worst teams, more teams with lower budgets are taking advantage of computational fluid dynamics as it is much cheaper for them than wind tunnel testing. Previously, they would only use CFD and because simulation time is limited in the F1 regulations, adding machine learning to speed up the testing process could be very crucial for those lower-budget teams to be able to do more simulations and get more data to match the teams with a higher budget that have access to wind tunnels and better CFD engineers. Increasing the competitiveness of F1 as a whole by setting all 10 teams on the same playing field in terms of aerodynamics technology could improve the viewing experience of hundreds of millions of fans around the world.

In addition to race cars, we also see the drastic effects of air pollution and the prevalence of gasoline use in road cars. According to Our World in Data in 2019, respiratory diseases caused by factors like air pollution was the third-leading cause of death globally. This life-threatening problem will only worsen in the future as at least 1.5 billion cars on the road will be petroleum-run in 2050, a 50% increase in the next three decades [6]. Without dramatically increasing the gas mileage of our daily vehicles with advanced technology from Formula One like optimized rear spoilers, cars will eventually lead to the Earth's collapse.

The application of the novel rear wing as well as the rear wing design and testing method to everyday road cars can also help us save the tens of millions of people that will die from respiratory diseases related to air pollution in the next few decades. Moreover, the fuel mileage increases that the rear wing can bring to cars will also make them much cheaper to operate, thus making cars more attractive to people that are wary about buying a new car, people that use other forms of transportation, and also people that cannot afford to purchase a car. This increased demand for cars with higher fuel mileage becomes even more apparent in the current world climate where rising gas prices are perpetually magnifying for a multitude of reasons, from geopolitical instability to oil scarcity.

Finally, this project is highly significant because although electric vehicles are a good alternative to reduce emissions, they are so unpopular across the world that they aren't making that large of an impact on car emissions reduction. For example, in Canada, only 5% of new cars bought in 2021 were electric [7]. This problem is only worsened in countries where the population is poorer on average. So, if buyers are unwilling to adopt new technology, adaptations to their current preferred option of gas-powered cars can be made with technologies like rear wings to make them more environmentally friendly to save millions of future generations from the ghastly effect of air pollution and climate change.

2. Methodology and Principles

2.1. Computational Fluid Dynamics (CFD)

There are two main research methods for fluid mechanics problems. First, there is the wind tunnel experiment. In wind tunnel experiments, researchers usually place the object to be studied in the wind tunnel, set boundary conditions such as the incoming flow velocity and outlet pressure, and then detect the flow field by adding dyes or sensors to the fluid.

The second method is CFD, a method that was just developed in the past few decades. Through computational simulations and experimentation based on the finite element algorithm, CFD calculates the pressure and velocity distribution of the flow field and then analyzes them. Although wind tunnel experimentation is a highly reliable research method, its operating cost is relatively high, making it infeasible as an option for this experiment. Moreover, it is wasteful to make multiple physical models of objects with minute differences just to keep testing with a wind tunnel.

Therefore, the latter research method was adopted for this research project. Currently, the development of CFD has been thorough, and the accuracy, reliability, and diversity of its algorithms can fully fulfill the requirements needed in a fluid mechanics research method for intensive academic research. Figures 3 and 4 show an F1 model car in a wind tunnel experiment and another CFD simulation, respectively.

Figure 3. F1 Car in Wind Tunnel Experiment

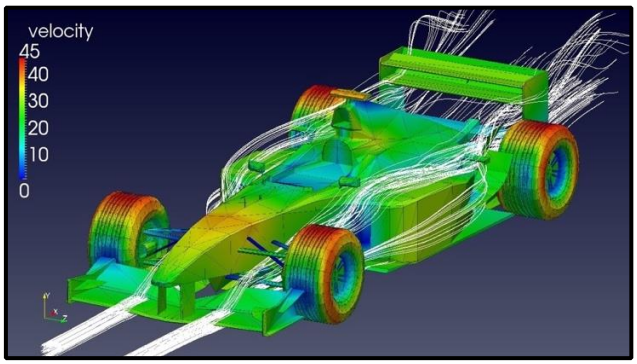

Figure 4. F1 Car Model in CFD Simulation

2.2. Fluid Mechanics Principles

In this section, governing equations of fluid mechanics are presented to explain how simulation results are found using software and how we can use those results to measure the performance of each simulated rear wing airfoil. Therefore, it is also necessary to display how these equations are derived and utilized in the simulation.

2.2.1 Law of Conservation of Mass

The Law of Conservation of Mass states that for an arbitrary control volume, the total mass entering the control volume must equal the total mass exiting the control volume plus the mass accumulating within the control volume. For example, in the control volume, as shown in Fig 5, the mass accumulating within the control volume is $\frac{\partial(\rho dxdydz)}{\partial t}$.

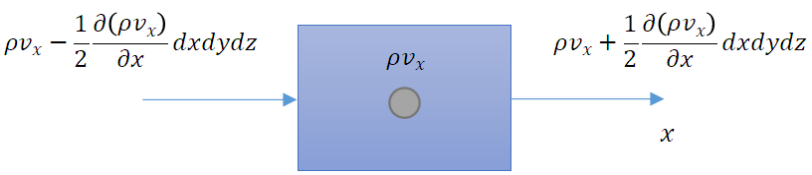

Fig 5. Using the x direction as an example to show mass conservation in an infinitesimal control volume

The net mass flux into the volume in the x, y, and z directions is the inflow rate minus the outflow rate, i.e.,$-\frac{\partial(\rho v_x)}{\partial x}dxdydz,\ -\frac{\partial(\rho v_y)}{\partial y}dxdydz, -\frac{\partial(\rho v_z)}{\partial z}dxdydz$, respectively. The sum of the net mass flux equals the accumulation within the control volume. For the cases of car moving, it is reasonable to assume that the air is an incompressible fluid, the density of the fluid is a constant, and the mass conservation could be expressed as:

$$\frac{\partial \mathrm{v_x}}{\partial \mathrm{x}} + \frac{\partial \mathrm{v_y}}{\partial \mathrm{y}} + \frac{\partial \mathrm{v_z}}{\partial \mathrm{z}} = 0 \tag{1}$$

2.2.2 Law of Momentum Conservation and Navier-Stokes Equations

The law of momentum conservation, which is namely a stretch of Newton's 2nd Law, can be deduced by expanding the equation of continuity along with Newton's 2nd Law. As this is a vector relation, it can be separated into forces on each of the three dimensions. In general, the forces that anticipate, including viscosity, pressure, and gravity, can be demonstrated in the following equations for streamwise, wall-normal, and spanwise directions, respectively,

$$\frac{\partial \mathrm{v_x}}{\partial \mathrm{t}} + \mathrm{v_x}\frac{\partial \mathrm{v_x}}{\partial \mathrm{x}} + \mathrm{v_y}\frac{\partial \mathrm{v_x}}{\partial \mathrm{y}} + \mathrm{v_z}\frac{\partial \mathrm{v_x}}{\partial \mathrm{z}} = -\frac{1}{\rho}\frac{\partial \mathrm{p}}{\partial \mathrm{x}} + \nu\left[\frac{\partial^2 \mathrm{v_x}}{\partial \mathrm{x}^2} + \frac{\partial^2 \mathrm{v_x}}{\partial \mathrm{y}^2} + \frac{\partial^2 \mathrm{v_x}}{\partial \mathrm{z}^2}\right] \tag{2}$$

$$\frac{\partial \mathrm{v_y}}{\partial \mathrm{t}} + \mathrm{v_x}\frac{\partial \mathrm{v_y}}{\partial \mathrm{x}} + \mathrm{v_y}\frac{\partial \mathrm{v_y}}{\partial \mathrm{y}} + \mathrm{v_z}\frac{\partial \mathrm{v_y}}{\partial \mathrm{z}} = -\frac{1}{\rho}\frac{\partial \mathrm{p}}{\partial \mathrm{x}} + \nu\left[\frac{\partial^2 \mathrm{v_y}}{\partial \mathrm{x}^2} + \frac{\partial^2 \mathrm{v_y}}{\partial \mathrm{y}^2} + \frac{\partial^2 \mathrm{v_y}}{\partial \mathrm{z}^2}\right] + \rho \mathrm{g} \tag{3}$$

$$\frac{\partial \mathrm{v_z}}{\partial \mathrm{t}} + \mathrm{v_x}\frac{\partial \mathrm{v_z}}{\partial \mathrm{x}} + \mathrm{v_y}\frac{\partial \mathrm{v_z}}{\partial \mathrm{y}} + \mathrm{v_z}\frac{\partial \mathrm{v_z}}{\partial \mathrm{z}} = -\frac{1}{\rho}\frac{\partial \mathrm{p}}{\partial \mathrm{z}} + \nu\left[\frac{\partial^2 \mathrm{v_z}}{\partial \mathrm{x}^2} + \frac{\partial^2 \mathrm{v_z}}{\partial \mathrm{y}^2} + \frac{\partial^2 \mathrm{v_z}}{\partial \mathrm{z}^2}\right] \tag{4}$$

These three equations are also collectively known as the Navier–Stokes equations.

2.2.3 Drag Coefficient

In fluid dynamics, drag (sometimes called resistance, a type of friction, or fluid resistance) is a force acting opposite to the relative motion of any object moving with respect to a surrounding fluid [8]. This can exist between two fluid layers (or surfaces) or a fluid and a solid surface. The drag coefficient (commonly denoted as C_d) is a dimensionless quantity that is used to quantify the drag or resistance of an object in a fluid environment. It is used in the drag equation in which a lower drag coefficient indicates the object will have less aerodynamic or hydrodynamic drag. The drag coefficient of any object comprises the effects of the two basic contributors to fluid dynamic drag: skin friction and form drag. In this study, the hydrophobic surface does not have a structured roughness shape and thus no form drag involved, so the study mainly focused on the skin friction drag of solid surfaces. The drag coefficient can be expressed as:

$$\mathrm{C_d} = \frac{\mathrm{F_d}}{\frac{1}{2}\rho \mathrm{u}^2 \mathrm{A}} \tag{5}$$

Here, C_d is the drag coefficient of the object, F_d is for the drag force on the object, ρ the density of the fluid, u is the reference velocity of the mainstream flow, and A is the frontal area of the object.

2.2.4 Lift Coefficient

Lift is the force that is perpendicular to the oncoming flow direction as either the mass of fluid around the object is moving or the object itself is moving in its surrounding fluid [9]. Objects that are heavier than their surrounding fluid generate lift using pressure differences. For example, airplane wings are designed to have the air flowing above them faster than the air flowing under them. From Bernoulli's equation, this creates a low-pressure area above the wing and a high-pressure area under the wing. By then turning the high-pressure region of air, lift is created. The lift coefficient (commonly denoted as C_l) is a dimensionless quantity that is used to quantify the lift that an object creates in a fluid environment. It is preferred by fluid dynamicists over simply the amount of lift an object creates because it accounts for differences in quantities like density across different environments for different airfoils.

$$C_l = \frac{F_l}{\frac{1}{2}\rho u^2 A} \quad (6)$$

Here, C_l stands for the lift coefficient of the object, F_l stands for the lift force on the object, ρ the density of the fluid, u is the reference velocity of the mainstream flow, and A is the frontal area of the object.

For flying aircraft, lift is used to move the aircraft upwards relative to its center but in race cars, lift is used to move the car downwards relative to its center, pointing toward the ground. This is because negative lift, more commonly known in the motorsport world as downforce, puts more vertical force on the tires to increase grip and traction, allowing them to be more stable and thus reach higher speeds around the track. This idea of negative lift also explains why rear wing airfoils on race cars look like inverted airplane wing airfoils.

2.3. Backpropagation Artificial Neural Network

Even though there are many artificial neural network models in the community, in this project, I used the Backpropagation Artificial Neural Network (BPANN) as it is one of the most widely applied neural network models. I would like to use this well-developed model as an example to show how the machine learning algorithm could be combined with the computational fluid dynamics tools to have a quick prediction. The BPANN algorithm, which usually includes a multi-layer feedforward network trained according to the error backpropagation algorithm, can construct the prediction model with greater accuracy and define the proportion of errors contributed by each factor to the aerodynamic forces. In BPANNs, backpropagation is used to regulate the weight value and threshold value, and usually, the steepest descent method is involved. By adopting the algorithm, the signal is processed first through the input layer, then the hidden layers, before it finally comes to the output layer. At the outer layer, the errors between the actual result and the predicted value are compared, which is further propagated backward to the hidden and input layers where the weights and thresholds are adjusted.

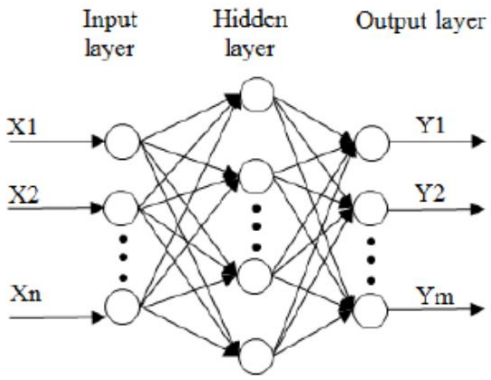

Figure 6. BP artificial neural network structure, including the three layers [10]

3. Airfoil Simulations

One of the most vital components of the project is data collection because, without sufficient and meaningful data, the machine learning model would not have accurately made correct predictions. So to collect data about some airfoils and their performances, ANSYS Fluent CFD software was used to simulate different NACA 63-412 rear wing airfoils.

3.1. Design of Test Airfoils

To design the 45 different sets of airfoil coordinates used in the CFD simulations, a website called airfoilstools.com was used, it can be accessed with the following link: http://airfoiltools.com/plotter/index. On the website, the default NACA 63-412 airfoil was altered to

create 45 different airfoil coordinates using 5 levels of thicknesses relative to the default NACA 63-412 airfoil's thickness: 50%, 100%, 150%, 200%, 250%, and 9 angles of attack (AOA): -20°, -15°, -10°, -5°, 0°, 5°, 10°, 15°, 20°. Figure 7 shows an example of an airfoil that was tested.

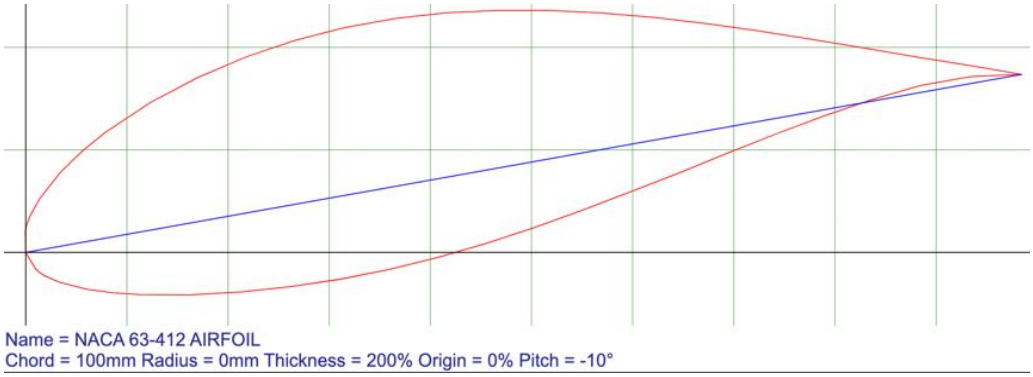

Figure 7. Example of tested rear wing airfoil design (200% thickness at -10º AOA)

3.2. Ansys Fluent Simulation Process

For each airfoil simulation, the process was to create the airfoil shape on ANSYS Fluent using 3D Cartesian coordinates, create a mesh to calculate the simulated area around the airfoil, configure the mesh to be highly precise, and then conduct simulations similar to airflow around an F1 car in real life. It then analyzes the simulation data to calculate its aerodynamic performance using complex fluid mechanics principles like the Law of Conservation of Mass and the Navier-Stokes equations to return the airfoil's drag and lift coefficients. Figure 8 shows the full mesh of a calculation domain with an airfoil that had a thickness of 250% of the base NACA 63-412 airfoil and an angle of attack of 0º.

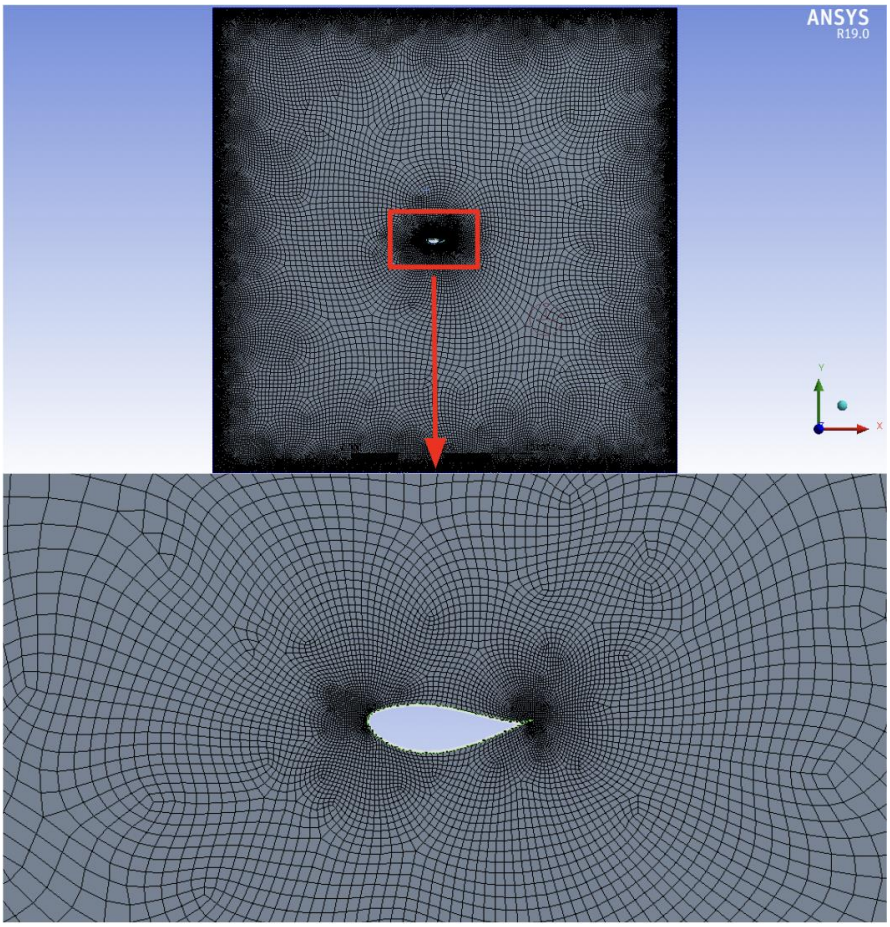

Figure 8. Full mesh of a calculation domain that was used in the project

3.3. Ansys Fluent Simulation Results

From analyzing one of the 90 simulations' results shown in figure 9, it can be seen that the airfoil entered a dynamic stall because of its large AOA. The airflow around the airfoil separated, forming a vortex (the blue circular region with low pressure and high velocity) at the leading edge of the airfoil (where airflow hits the airfoil first) that travelled back to the trailing edge of the airfoil (where airflow leaves the airfoil). Stalls stop wings from creating any positive lift or downforce. The airfoil in figure 10 would make a good F1 rear wing because it forms a low-pressure region below it and a relatively higher pressure region above it, pushing the wing down to the floor, and creating downforce. The airfoil accomplishes this because of Bernoulli's principle, an increase in the speed of a fluid occurs simultaneously with a decrease in static pressure. The airfoil is shaped so that air flows faster below it compared to above it.

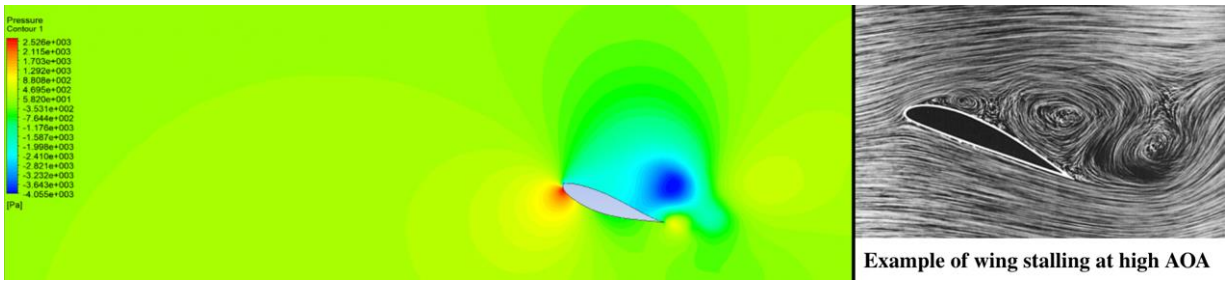

Figure 9. CFD pressure contour results of an airfoil as the wing is stalling

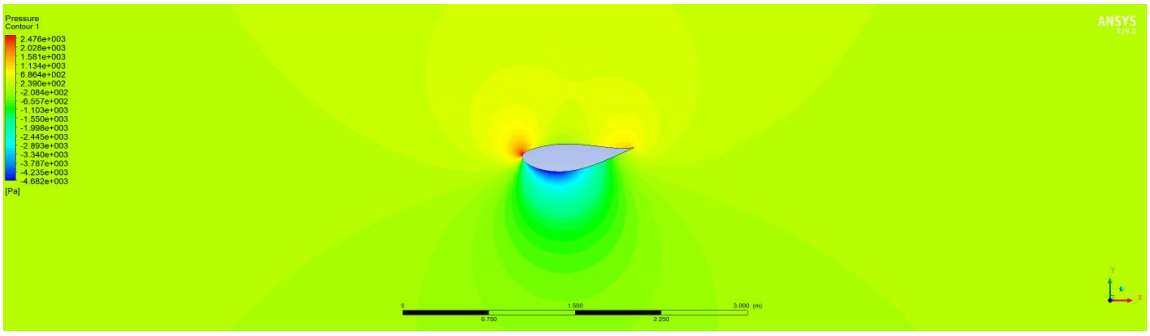

Figure 10. CFD pressure contour results of an airfoil that would create high downforce

To account for minor errors, each airfoil, each pair of lift coefficient and drag coefficient values that were calculated in the last 50 iterations of the CFD simulation were averaged using MATLAB and used as the final aerodynamic performance values of that airfoil. Those performance values were with the parameters of the airfoil that produced those values. The first 6 simulations' data is shown in table 1.

Table 1. Data from the first 6 CFD simulations

Simulation Number	Thickness (%)	Angle of Attack (°)	Velocity (m/s)	Drag Coefficient	Lift Coefficient	Lift/Downforce to Drag Ratio
1	250	0	33	0.0238	-0.7521	-31.60084034
2	250	0	66	0.0223	-0.7702	-34.53811659
3	250	5	33	0.0262	-0.1882	-7.183206107
4	250	5	66	0.0248	-0.1977	-7.971774194
5	250	10	33	0.0365	0.1281	3.509589041
6	250	10	66	0.0347	0.1403	4.043227666

3.4. Machine Learning Results and Discussion

Although an adequate understanding of airfoil parameters like angle of attack (AOA) and thickness was established in relation to airfoil performance, the best-performing airfoils from the 90 simulations could still be improved with thousands of more simulations. However, since that would take hundreds of hours, a machine learning model was used. The model used data collected from the 90 previous simulations as a basis. Then, it predicted simulation results in a fraction of the time it took ANSYS Fluent while still maintaining high accuracy rates. Machine learning found the most optimal design for an F1 rear wing to very precise parameter values and created graphs that modelled each airfoil's performance relative to any parameter.

The Backpropagation Neural Network Algorithm includes forward propagation and backpropagation, in which the gradient descent method is adopted to regulate the weight value of all layers. In this process, when a set of inputs corresponds to a set of outputs, the internal process occurs within the computer. The computer keeps adjusting the weights and the threshold in each layer of neurons so that the input value can predict with the slightest difference compared to the actual value. The detailed formulation of the Backpropagation Neural Network Algorithm could be found in the literature [11].

The machine learning model was highly accurate because the graph that was used to train the model to create an algorithm showed an R^2 value of 0.92282, as shown in figure 11. R^2 is a measure of how close predicted values are to actual values. 0 means there is no correlation between all predicted and actual values while 1 represents a perfect correlation. With this high accuracy, three predictions were made using the data from the ninety ANSYS Fluent simulations. Using the ratio C_l/C_d instead of only C_l or only C_d to measure airfoil performance ensures that the most optimal airfoil creates both high downforce and low drag, avoiding airfoils that create high downforce but high drag or airfoils that create low drag but low downforce.

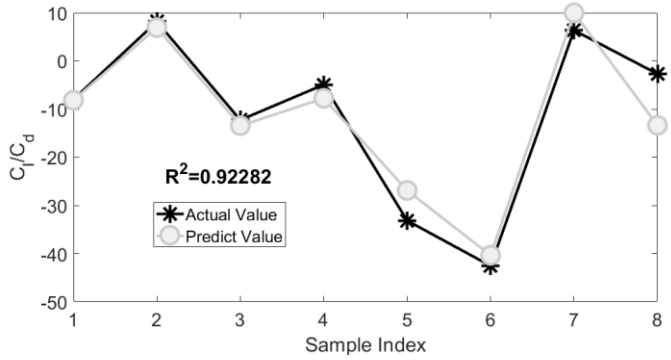

Figure 11. Testing accuracy of the model in predicting C_l / C_d values

In figure 12, the first machine learning simulation, velocity was fixed at 33 meters per second (m/s) and the AOA at 0º. The most optimal airfoil's thickness was found to be approximately 175% the thickness of a base NACA 63-412 airfoil because it is predicted to have the lowest C_l/C_d value, meaning it would produce the most negative lift (downforce) relative to drag creation.

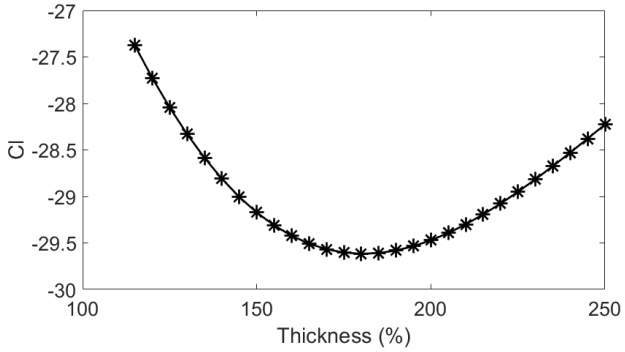

Figure 12. Predicted most optimal thickness level of NACA 63-412 of an airfoil in motion

In figure 13, the second machine learning simulation, velocity was fixed at 33 m/s and thickness at 175%. The most optimal airfoil's AOA was found to be at approximately -4º, which also means 4º below the horizontal.

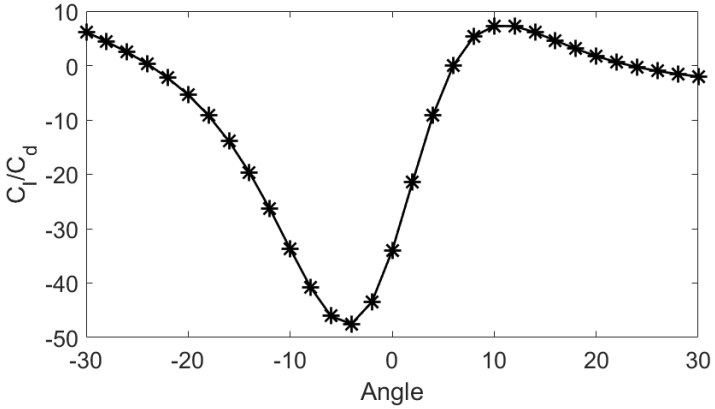

Figure 13. Predicted most optimal angle of attack (º) of an airfoil in motion

In figure 14, the third machine learning simulation, the thickness was fixed at 175% and AOA at -4º. The most optimal airfoil would perform the best when the race car travels at approximately 90 m/s.

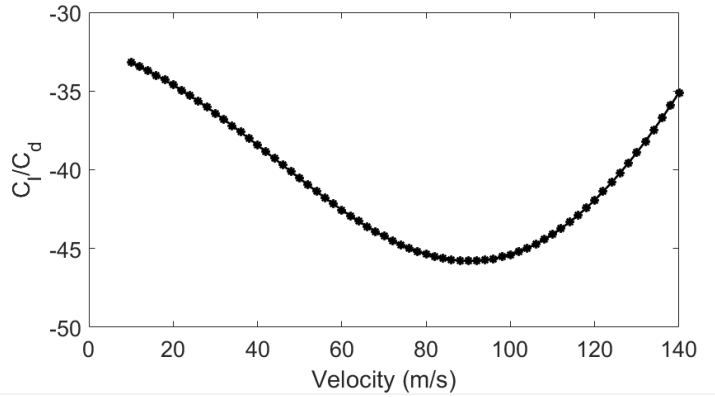

Figure 14. Predicted most optimal flow velocity of an airfoil in motion

4. Amalgamation of Optimized Rear Wing and F1 Race Car

In the final stage of the project, following the interpretation of all the machine learning model's outputs, the theorized most optimal airfoil for an F1 race car was tested in CFD, given the impracticality of real-world wind tunnel testing, after being amalgamated to the rest of a model F1 car.

4.1. F1 Race Car Development

To start, SolidWorks, a design and modelling software for Computer-Aided Design (CAD) was used to design a base F1 car model that was later used for simulations and analysis. To make the optimized rear wing, the coordinate points of it on a standard 2D cartesian plane were found using the same website that was used to design the 45 airfoils used in the first round of CFD simulation. Then, those coordinate points were put into an Excel sheet, changed to fit the data input format that SolidWorks uses, uploaded in tabular form onto SolidWorks, and SolidWorks formed a 2D model of the airfoil from the input data. Finally, the 2D shape was extruded to the length of an F1 rear wing and fit on the base F1 race car model. Figure 15 shows a side-by-side comparison of the base and completed CAD models of the F1 race car. The car on the left does not have a rear wing, and the car on the right has the optimized rear wing.

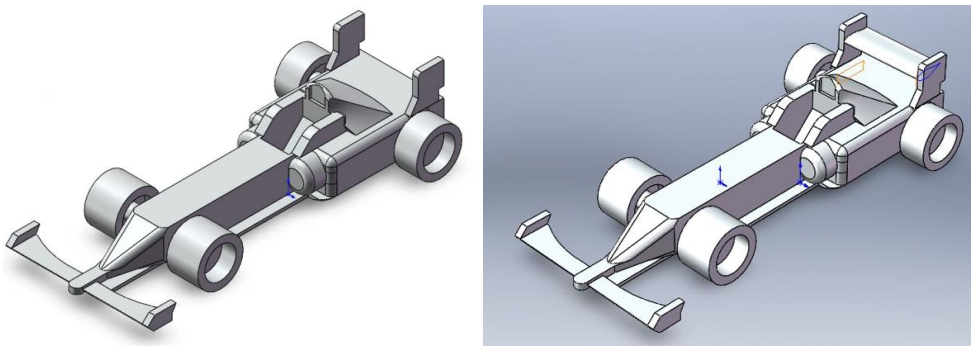

Figure 15. F1 race car CAD model (Left: Base model, Right: Optimized model)

4.2. Implementation of Optimized Rear Wing

Following the creation of the rear wing using the optimized airfoil and its attachment to the base F1 car, 3D ANSYS Fluent simulations were conducted to compare an F1 race car with no rear wing and another with the optimized rear wing. The results of the simulations, shown in figure 16, explain that the SolidWorks model F1 race car without a rear wing has a C_l of 0.7362 and a C_d of 0.9865 while the model F1 race car with a 175% thickness NACA 63-412 airfoil set at -4º AOA and 33 m/s velocity has a C_l of 0.6837 and a C_d of 0.5619. Figure 17 shows the visualized data from both simulations.

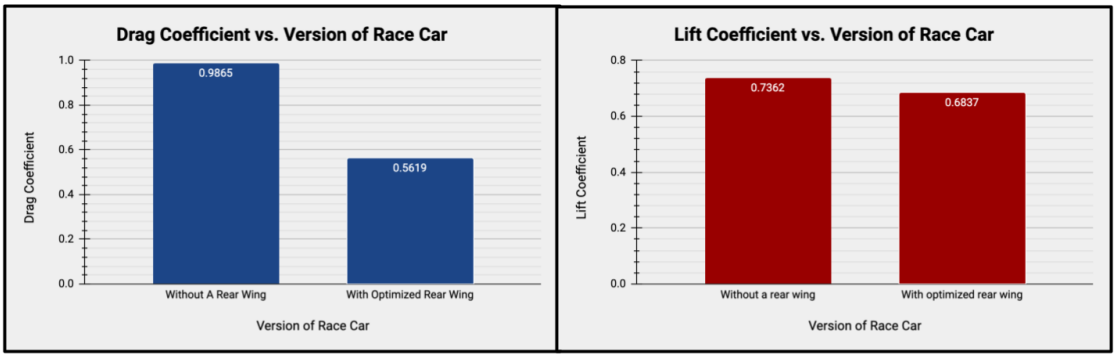

Figure 16. Results of 3D CFD simulations

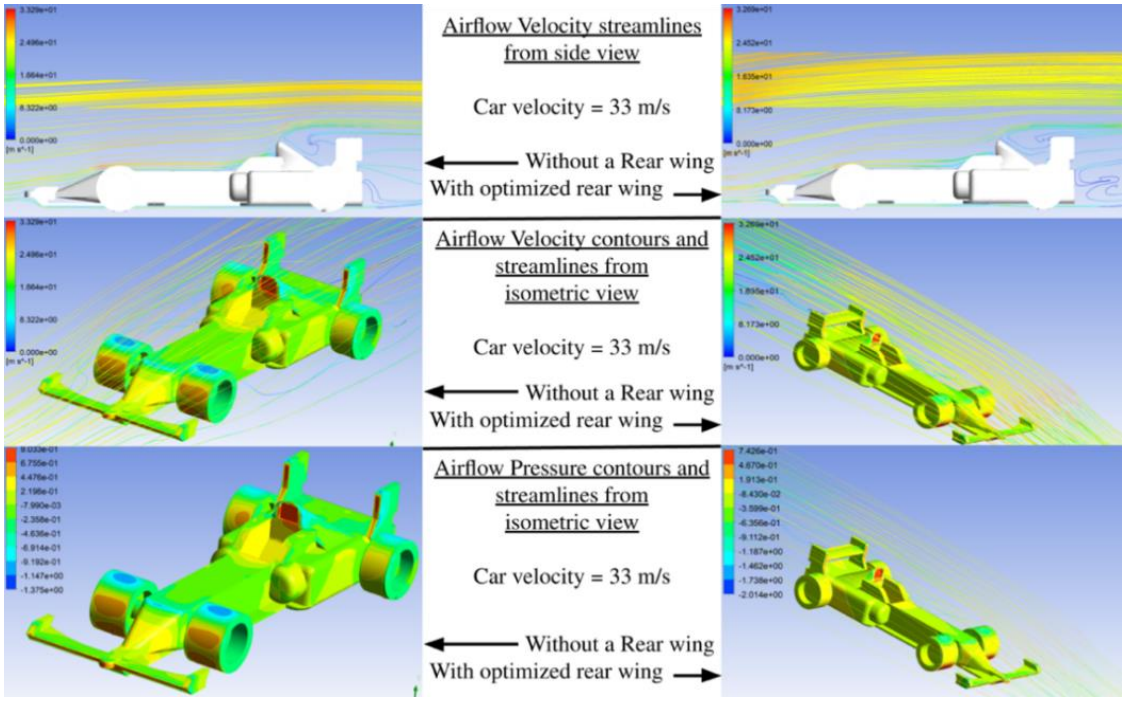

Figure 17. Visual comparisons between both race cars using simulation contours and streamlines

4.3. Results and Discussion of Race Car Simulation

The increased downforce caused by the optimized rear wing is significant because downforce creates more grip and thus more speed and acceleration. The decrease in drag coefficient attributed to the rear wing is important because, for road cars, a 43.04% decrease in the car's total drag coefficient improves a car's highway fuel economy by 21.52%, a notable economic and environmental benefit.

These aerodynamics improvements were found by optimizing F1-specific airfoils and testing with an F1 race car but optimizing and testing road car-suited spoilers could yield even greater enhancements.

Finally, F1 technology is often used by companies who produce popular road cars to help make better cars for the average driver as well. For example, the Kinetic Energy Recovery System, or KERS, was developed in Formula One to convert energy wasted from braking to 80 brake horsepower for the race car to use when speeding down the straights [12]. From this innovation, in 2020, the popular car manufacturer, Volvo, redesigned their XC90 model to implement a KERS, which saw increases in fuel economy by 15% compared to their old XC90 model [13].

Using Volvo's KERS implementation as a reference, with the further research of rear wing airfoils in this project to road-legal cars, everyday drivers can also enjoy the benefits found in the results, lower fuel consumption and higher mileage, positively contributing to the world for many generations to come.

5. Conclusion and Future Work

5.1. Conclusion

In this research project, I focused on how the performance and research and development stage of race cars and road cars can become faster, more efficient, and cheaper to positively impact the world. I used CAD, CFD, and machine learning tools to not only develop a novel F1 race car rear wing but also to innovate a novel design, research, and testing process for rear wings, which can also be adapted for all major exterior car parts. The final and most important quantitative conclusions from the project are that firstly, the most optimal rear wing airfoil for an F1 race car has a 175% thickness relative to the default NACA 63-412 airfoil, and it is set at a -6º angle of attack, and secondly, the use of a rear wing made from this airfoil on an F1 race car creates a 43.04% drag reduction and 7.131% downforce production relative to an F1 race car without a rear wing.

5.2. Future Work

With a larger budget, this project could have been done with wind tunnel experimentation. To do so, the airfoil would be 3D printed. Then, after setting the wind flow velocity and pressure, by adding dyes or sensors to the fluid, the airflow around the airfoil would be detected and analyzed.

Furthermore, seeing the significance of the project's results quantitatively and its potential to be useful in the real world, I will pursue future car development with road car companies for the environmental, commercial, and economic benefits that the novel research and design method can bring.

Environmentally, because millions of people die from respiratory diseases related to air pollution as well as natural disasters from climate change, I hope that by reaching out to car companies to implement my project's innovative methods, I can tackle those problems head-on to save future generations.

Commercially, by increasing the fuel mileage of cars through spoilers and rear wings created through the fast and easy testing methods, cars will be more attractive to people that don't have or cannot purchase a car right now, helping the companies make more money to funnel back into research and development for even better cars in the future.

Economically, new cars with higher fuel mileages saves people thousands of dollars annually, even without factoring in the ongoing global inflation and rising gas prices. Additionally, I want to introduce my novel method to Formula One. Crucially, poorer teams would be able to more efficiently upgrade their cars to catch up to the richer teams, which closes the performance gap between them. This increases competitiveness, and thus helps F1 become more popular to billions of people around the world.

References

[1] Formula One. (2021, February 8). Formula 1 announces TV and Digital audience figures for 2020 | Formula 1®. https://www.formula1.com/en/latest/article.formula-1-announces-tv-and-digital-audience-figures-for-2020.3sbRmZm4u5Jf8pagvPoPUQ.html

[2] Fagnan, R. (2018, January 31). The first appearance of wings on Formula 1 cars. Motorsport.Com. https://us.motorsport.com/f1/news/1968-first-wings-f1-1000902/1389076/

[3] Reddy, J. Jagadeep, and Mayank Gupta. "Finding the optimum angle of attack for the front wing of an F1 car using CFD." In Proceedings of the 4th WSEAS International Conference on Fluid Mechanics and Aerodynamics, pp. 29-34. 2006.

[4] Ravelli, U., & Savini, M. (2018). Aerodynamic simulation of a 2017 f1 car with open-source cfd code. J. Traffic Transp. Eng, 6.

[5] Patel, M. (2021, April 10). Explained: How Formula 1 is aiming to go carbon neutral by 2030. The Indian Express. https://indianexpress.com/article/explained/explained-how-formula-1-is-aiming-to-go-carbon-neutral-by-2030-7267582/

[6] Fuel Freedom Foundation. (n.d.). https://www.fuelfreedom.org/cars-in-2050/. https://www.fuelfreedom.org/cars-in-2050/

[7] Rabson, M. (2022, April 22). Canadian EV sales grew in 2021 but are not on track for federal targets. Automotive News Canada. https://canada.autonews.com/electric-vehicles/canadian-ev-sales-grew-2021-are-not-track-federal-targets

[8] Wikipedia. (2022a, August 19). Drag (physics). https://en.wikipedia.org/wiki/Drag_(physics)

[9] Wikipedia. (2022b, August 22). Lift (force). https://en.wikipedia.org/wiki/Lift_(force)

[10] Thanasarn, T., & Warisarn, C. (2013, August). Comparative analysis between BP and LVQ neural networks for the classification of fly height failure patterns in HDD manufacturing process. In Proceeding conference paper ICEAST (p. 4).

[11] Li, J., Cheng, J. H., Shi, J. Y., & Huang, F. (2012). Brief introduction of back propagation (BP) neural network algorithm and its improvement. In Advances in computer science and information engineering (pp. 553-558). Springer, Berlin, Heidelberg.

[12] Racecar Engineering. (2011, January 27). The basics of F1 KERS. https://www.racecar-engineering.com/articles/the-basics-of-f1-kers/

[13] Sergeev, A. (2019, February 22). Volvo XC90 Facelift Unveiled with KERS For Better Fuel Efficiency. Motor1.Com. https://www.motor1.com/news/306472/volvo-xc90-facelift-revealed/